Exercizing the Chandra Grating Line Response Functions: HETGS and Capella

Sun Mi Chung, Jeremy Drake, Vinay Kashyap

October 20, 2003

Summary

As part of a more comprehensive study to better understand the line response function (LRF) of the Chandra transmission grating spectrographs (LETGS and HETGS), we present results from a study of an in-flight calibration observation (Capella ObsID 2583) and cycle 5 response matrix files (RMFs) of the HETG. This study was undertaken before the LETG+HRC-S case because of known imaging non-linearity problems in the latter that complicate line profile analysis.

By comparing the observed line profiles of Capella with theoretical profiles that are broadened by thermal, rotational, and instrumental broadening mechanisms, we have learned that the cores of the RMF profiles provide reasonable approximations to the actual instrument behavior, while the wings of the RMFs appear to be too narrow. If we compare the observed profiles to the core of the theoretical profiles (by taking the analytical FWHM), we find that the rms deviation of the observed line widths to the theoretical line widths are $\sim 11\%$ for MEG and $\sim 12\%$ for HEG. There is an apparent tendency for the RMF to slightly overestimate the actual core FWHM toward longer wavelength RMF.

We have also found that the negative order and positive order Capella profiles show evidence for systematic differences in measured line widths, with negative order lines appearing slightly broader. The line widths are usually within 2σ, except in the case of MEG Mg XII (8.42 Å), which shows a difference of 2.6σ.

1 Observations

If we are to accurately predict the line profiles of a given source, it is important that we have a good understanding of the thermal and non-thermal broadening that define the intrinsic source line profile. We also need a source whose spectrum shows lines of high signal to noise ratio (S/N) over a broad range of wavelengths in order to thoroughly test the LRF. For these reasons, Capella serves as an excellent source to examine LRF; it is the brightest narrow line source in the X-ray sky, has been very well-studied, and exhibits strong lines over most of the range of the HETGS. In addition to high S/N lines, we need lines that are fairly unblended; line blends can distort the observed profile, and are more difficult to accurately model. A list of relatively unblended lines in the Capella spectrum was generated by computing model spectra and taking only those lines whose blending fractions were not expected to exceed 10%.

We intentionally chose the ACIS-S+HETG Capella observation ObsID 2583, which was observed in April of 2002, with an exposure time of 28 ks. At that time, the two giants were near conjunction in phase and line broadening due to the orbital velocity of both binary components was, to all intents and purposes, eliminated.

We also measured the line widths of an ACIS-S+HETG observation of another very bright coronal source, Algol (ObsID 604). Algol presents an interesting challenge for line profile analysis because the Doppler shifts associated with the orbital motion of Algol B (thought to be responsible for all the observed X-ray flux) should be easily observable with the HETG. To test line profiles we first remove this component by correcting photon positions in the evt2 file according to the optical ephemeris. We use this observation to compare the line widths of the positive, negative, and coadded orders. ObsID 604 was observed in April of 2000 with an exposure time of 52 ks.

In all cases, data processed with pixel randomization switched on was used; this corresponds to released RMF's, which were derived based on simulations that included pixel randomization.

2 Constructing Theoretical Line Profiles

Theoretical line profiles were constructed for strong lines which optically-thin plasma model calculations indicated to be relatively free from blends.

These lines are listed in Table 4. We computed theoretical profiles by convolving thermal, rotational, and instrumental line broadening components.

In 2001, Young et al. examined the Capella spectrum observed with FUSE (Far Ultraviolet Spectroscopic Explorer) with a resolving power of $\lambda/\Delta\lambda = 10,000$—ten times the Chandra HETG resolution—and found that a theoretical line profile of the forbidden Fe XVIII 976 Å coronal line described only by thermal, rotational, and instrumental line broadening, was well matched to the observed profile. We therefore feel reasonably confident that the intrinsic line profiles of Capella are significantly broadened only by thermal and rotational broadening. This is important for this LRF study: significant discrepancies between theoretical and observed line profiles would therefore be caused by a problem with the predicted instrumental broadening.

The thermal profile for each ion is derived by constructing individual thermal profiles for an array of temperatures. Each profile for a given temperature is a gaussian of width $\sigma = \sqrt{\frac{2kT}{m}}$, where k is the Boltzmann constant, T is the ion temperature, and m is the ion mass. The final thermal width of a given ion is calculated as the weighted average of the individual thermal widths computed at various temperatures, where the weighting function is the product of the emission measure and the line emissivity at each temperature. The emission measure distribution used was also derived from HETG Capella observations using a new H-/He-like line ratio method.

The rotational broadening was derived by assuming a spherically symmetric solid body model with a rotational velocity of the slower moving G8 star, at 3 km/s. We have chosen to use the rotational velocity of the slower moving G8 giant to be consistent with Young et al. (2001), who found that the G8 star dominates the Fe XVIII profile. However, we will note that choosing the rotational velocity of either star has negligible effect on the FWHM of the theoretical profile.

We then convolve the thermal and rotational profiles with the RMFs to obtain our final theoretical profiles.

To characterize the line widths of the observed profiles, we fit the lines listed in Table 4 with a modified Lorentzian function of the form $F(\lambda) = a/(1 + (\frac{\lambda-\lambda_0}{\Gamma})^2)^\beta$, where a is the amplitude and Γ is a characteristic line width , with a value of 2.5 for β. We used this value of β because in 2001, Drake et al. showed that when fitting ACIS-S+LETG data, a β value of 2.5 results in the best fit. We show that this is also true for ACIS-S+HETG data (Figure 3).

3 Observed versus Theoretical Line Profiles

Figure 2 shows the Fe XVII line from the Capella spectrum with the plus and minus orders coadded, overplotted with the theoretical profile of Fe XVII. We can see that the theoretical profile does a good job at approximating the core of the observed line, but a poor job at approximating the wings. The wings of the theoretical profiles are much too narrow to match the data. While this additional broadening could simply be the result of errors in continuum location, or the combined effect of the blending of several weak lines, we feel these explanations are unlikely: the same trend is seen in all lines analysed.

We can characterise this effect to some extent by comparing predicted and observed line profiles to modified Lorentzian functions. Figure 3 illustrates goodness-of-fit (χ^2) as a function of the exponent β in the modified Lorentzian function previously discussed. The observed O VIII profile is best fit by $\beta = 2.5$, while the theoretical O VIII profile is best fit by a much higher asymptotic value of β. Increasing β leads to less extended wings—this trend is then expected if the wings of the RMF are too narrow to simulate actual instrument behavior. Because the wings of the RMF are too narrow to match the data, fitting the theoretical profiles with a modified Lorentzian of $\beta = 2.5$ yields line widths that significantly differ from the actual widths of the theoretical profiles (determined numerically).

Table 4 lists the measured FWHM of the observed and theoretical profiles (measured by fitting modified Lorentzians with $\beta = 2.5$), and the analytical FWHM of the theoretical profiles. There is fairly good agreement between the observed FWHM and the analytical FWHM of the theoretical profiles (up to 2.3σ in the MEG data), but poor agreement between the measured FWHM of the data versus the measured (fitted) FWHM of the theoretical profiles (up to 7.7σ). We attribute this to the core of the RMFs being well-matched to the actual data, but not the wings. The modified Lorentzian with $\beta = 2.5$ is a sufficiently bad match to the theoretical profiles, such that fitting this profile leads to a systematically small FWHM: the FWHM needs to be smaller so as to accomodate the wider wings of the modified Lorentzian.

On average, the measured FWHM of the MEG data fall within 1.3σ of the analytical FWHM of the theoretical profiles (1.1σ for HEG). Figure 1 compares the measured FWHM of the data to the analytical FWHM of the theoretical profiles for the negative, positive, and coadded order lines of Capella. The rms deviation of the negative and positive order residuals shown in Figure 1 is $\sim$ 11% for MEG, and $\sim$ 12% for HEG. Notice that for lines of longer wavelengths, the theoretical profiles become increasingly too broad in comparison to the observed data, indicating that the RMFs are too broad at smaller energies.

4 Negative versus Positive Order Spectra

Through a comparison of positive and negative order line profiles, we hav uncovered a discrepancy between the plus and minus order line widths in the Capella ACIS-S+HETG observation. Figure 4 shows the negative and positive order profiles of O VIII. The two profiles clearly show different wavelength centroids which we attribute to small calibration errors in chip gaps and/or errors in location of the 0th order centroid.

To characterize the differences in plus and minus order spectra, we have measured the line widths of the six emission lines listed in Table 4 for data in both orders, as well as for coadded data. The coadded spectrum was obtained by first measuring the wavelength centroids of the lines in the plus and minus orders, then shifting one spectrum relative to the other such that the wavelength centroids of the two orders are the same. Figure 5 shows the measured FWHM of the plus, minus, and coadded spectra, for an observation of Algol (ObsID 604) and Capella (Obsid 2583). The Algol plus and minus order line widths agree within $\pm\ 1.5\sigma$. However, the Capella data show differences between plus and minus order line widths of up to 2.6σ.

At present, it is unclear what could be causing these line width differences in Capella but not in Algol. We do not believe that chip gaps are the cause of this observed discrepancy between plus and minus orders. For example, the MEG positive order Ne X line (12.13 Å) in Capella falls on a chip gap, yet the plus and minus order line widths are in agreement within 1σ. One explanation could be the alignment of the ACIS-S detector: we would expect to begin to see significantly different line widths if one side of the detector were raised or lowered relative to the Rowland circle by of order 100 μ or so. A study of of the in-flight focusing observations would be warranted to investigate such a possibility, though it might also be possible that such an effect could have developed in the intervening two or so years of operation that separate the in-flight focussing test and the Capella observation analysed here.

That the effect is not obvious in Algol might be simply due to the Algol profiles being intrinsically broader than those of Capella. We note that the

Algol observation was performed two years before the Capella observation analysed here: again this raises the possibility of a drift in the negative order line widths over the intervening years.

Table 1: The first column lists the laboratory wavelengths of the lines we have analyzed for Capella (ObsID 2583), followed by the measured FWHM of the negative, positive, and coadded data. The next two columns list the analytical FWHM of the theoretical profiles, and the measured FWHM of the theoretical profiles (which were fitted with a modified Lorentzian with $\beta = 2.5$).

Wvl Å	measured FWHM(-ve)	measured FWHM(+ve)	measured FWHM(coadd)	analytical FWHM(theory)	measured FWHM(theory)
MEG					
24.78	0.0262 ± 0.0071	0.0094 ± 0.0085	0.0236 ± 0.0056	0.0264	0.0214
18.97	0.0226 ± 0.0011	0.0185 ± 0.0019	0.0223 ± 0.0009	0.0236	0.0192
16.78	0.0197 ± 0.0009	0.0178 ± 0.0013	0.0195 ± 0.0007	0.0211	0.0172
15.01	0.0204 ± 0.0006	0.0185 ± 0.0009	0.0208 ± 0.0005	0.0197	0.0168
12.13	0.0214 ± 0.0009	0.0205 ± 0.0009	0.0216 ± 0.0006	0.0212	0.0176
8.42	0.0236 ± 0.0018	0.0183 ± 0.0010	0.0208 ± 0.0009	0.0195	0.0175
HEG					
12.13	0.0160 ± 0.0012	0.0163 ± 0.0015	0.0166 ± 0.0008	0.0139	0.0104
8.42	0.0138 ± 0.0019	0.0124 ± 0.0014	0.0132 ± 0.0010	0.0129	0.0101

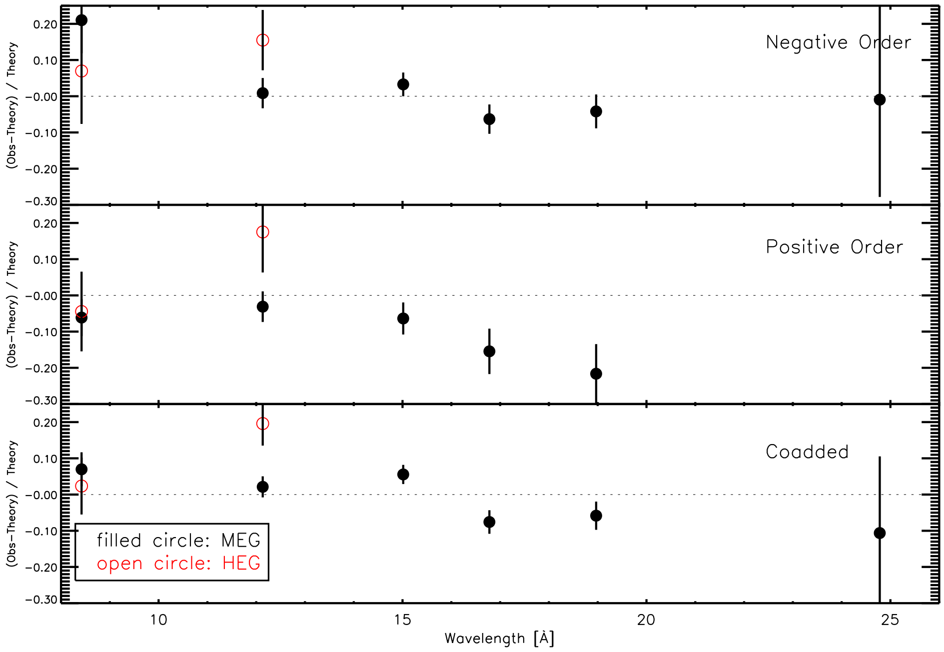

Figure 1: Plot of the observed minus theoretical FWHM divided by the theoretical FWHM (along with 1σ error bars), for various lines in the negative order (top), positive order (middle), and coadded order (bottom) Capella data. The filled circles represent the MEG residuals, and the open circles represent HEG. Note that for longer wavelengths, the data seem to drift further away from the zero-point (dotted line).

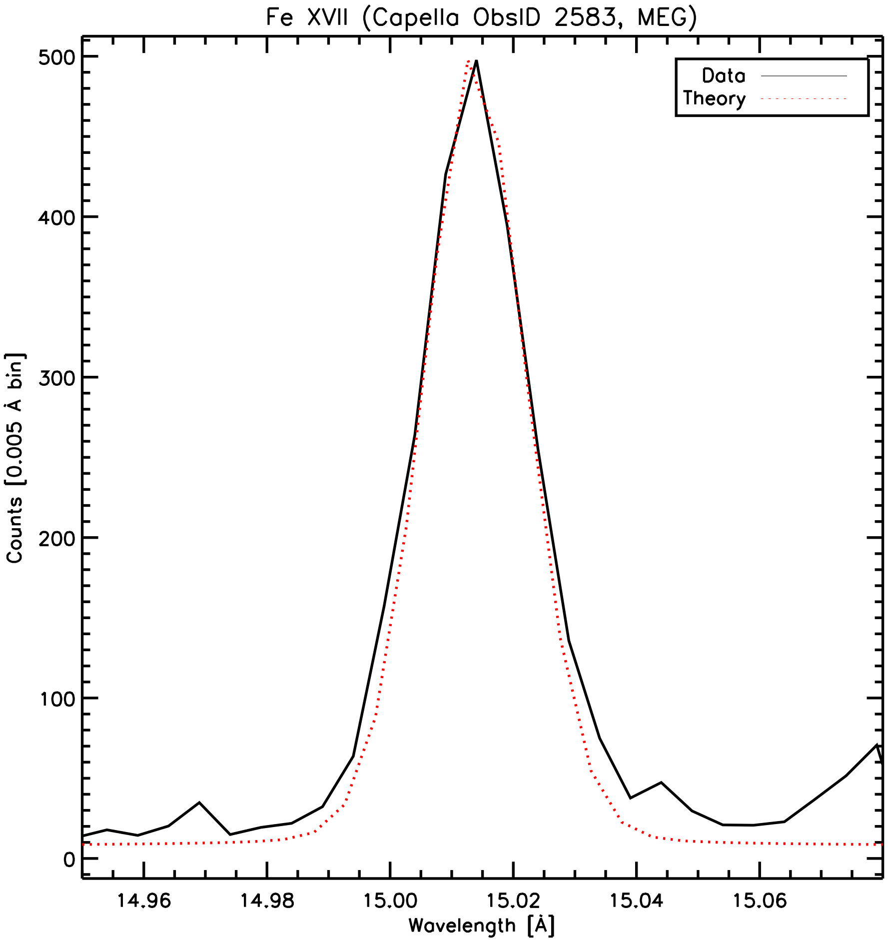

Figure 2: Plot of the Fe XVII Capella line profile (plus and minus orders coadded), with the theoretical line profile overplotted (dotted line). While the core of the theoretical profile is a good estimate for the observed data, the wings are too narrow.

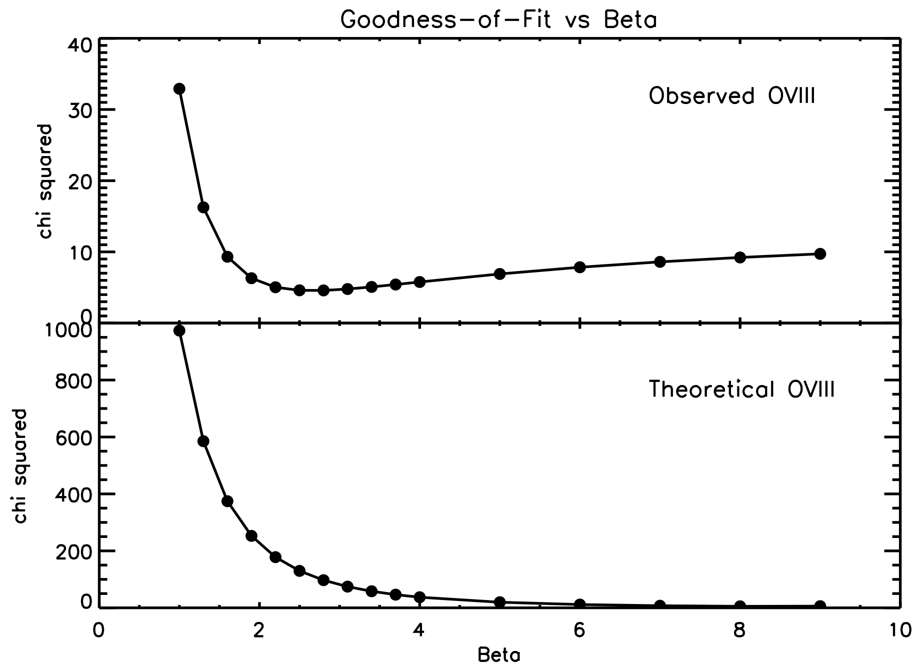

Figure 3: Illustrates the goodness-of-fit (χ^2) as a function of β, for observed and theoretical O VIII profiles. The best fit for the observed data occurs near $\beta = 2.5$, while the best fit for the theoretical profile requires a much higher value of β to account for its more narrow wings.

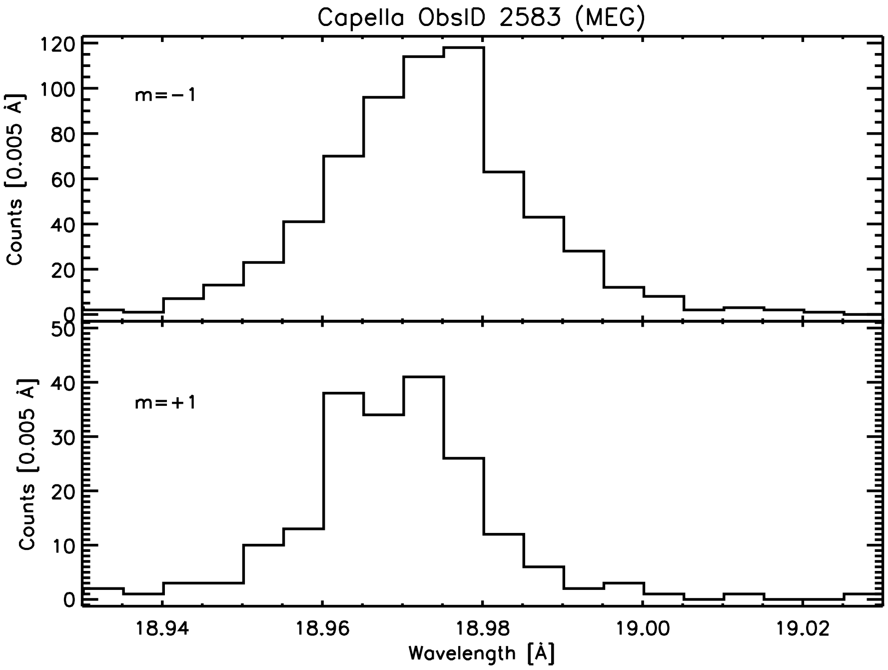

Figure 4: Shows the MEG O VIII profile of Capella, in both the plus and minus orders. The two profiles show significantly different wavelength centroids and line widths.

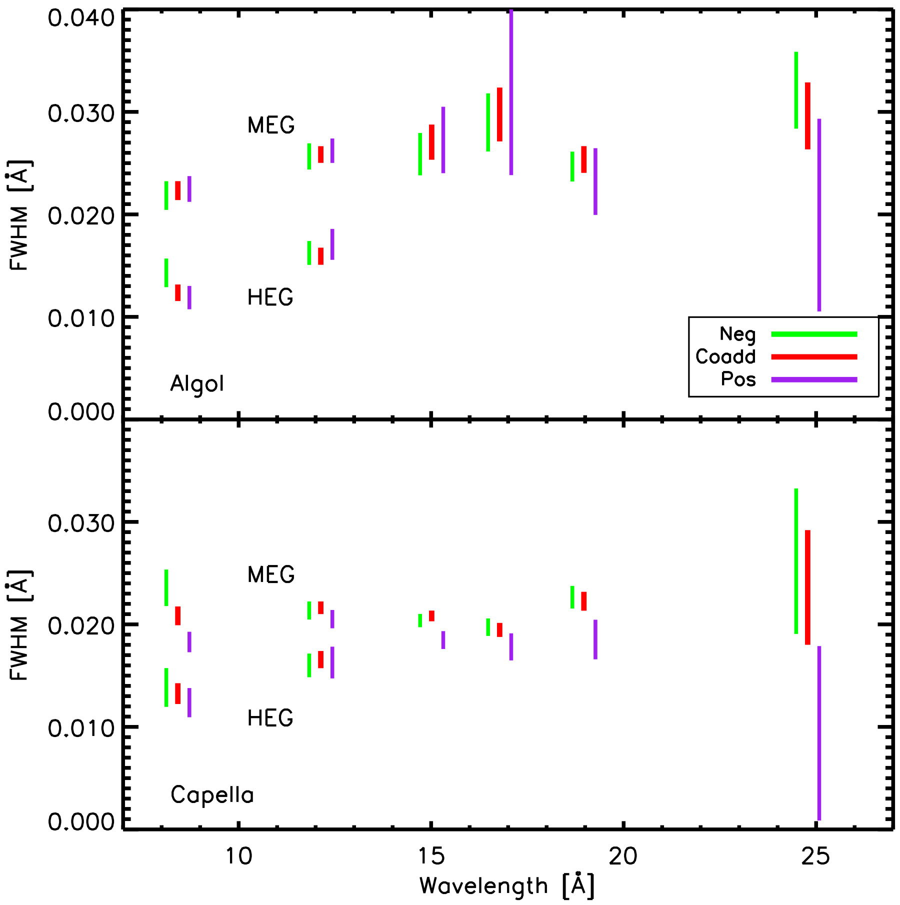

Figure 5: The measured FWHM of lines from plus, minus, and coadded orders. FWHM are shown for both Algol and Capella, in HEG and MEG. In general, the Algol data show better agreement between the plus and minus order line widths, which are all within 1.3σ. The Capella plus and minus order line widths agree within 2σ, with the exception of the MEG Mg XVII (8.42 Å) line, which agree within 2.6σ.

References

- Young, P. R., Dupree, A. K., Wood, B. E., Redfield, S., Linsky, J. L., Ake, T. B., Moos, H. W.

  2001, ApJ, 555, L121

- Drake, J. J.

  2001, Calibration Review

  http://asc.harvard.edu/cal/Links/Letg/User/Review_311001/imaging.html